

## Dynamical simulation of a quantum harmonic oscillator in a noble-gas bath by density-matrix evolution

Janez Mavri\* and Herman J.C. Berendsen†

*BIOSON Research Institute, Department of Biophysical Chemistry, The University of Groningen, Nijenborgh 4, 9747 AG Groningen, The Netherlands*

(Received 15 April 1993)

A density-matrix evolution method [Berendsen and Mavri, *J. Phys. Chem.* **97**, 13 464 (1993)] coupled to a classical molecular dynamics simulation was applied to study a quantum harmonic oscillator immersed in a bath of Lennard-Jones particles. Eigenfunctions of the three lowest levels of the unperturbed oscillator were used as basis functions. Time-averaged populations of vibrational levels obey Boltzmann's distribution law. In the calculated vibrational spectrum asymmetric peak broadening associated with blueshift is observed in a dense argonlike bath.

PACS number(s): 05.30.-d, 02.70.Ns, 03.65.Sq, 34.30.+h

### I. INTRODUCTION

Molecular dynamics (MD) simulation is a valuable tool for the calculation of equilibrium and nonequilibrium statistical mechanical quantities, especially for systems that are too complicated for analytical treatment. Classical MD simulations are based on the premise that particles being simulated are described with sufficient accuracy by the laws of classical mechanics. However, there are many systems of interest for which classical mechanics provides a sufficiently accurate description of the motion for almost all the degrees of freedom, while for a small number of degrees of freedom a quantum mechanical description is required. Quantum treatment of all degrees of freedom would be impractical, even using the most powerful computers.

The path integral (PI) method can blend classical and quantum degrees of freedom and yield quantum dynamics [1]. The traditional view of the PI method is that it is not able to predict quantum dynamics due to numerical difficulties in the calculation of the multidimensional phase integral [2]. The large phase cancellation makes the integral calculation extremely difficult. However, recently progress has been reported for some systems [3–6]. The traditional application of PI where the quantum particle is described as a closed necklace of beads gives only correct ensemble averages but cannot be considered as a quantum dynamical method.

The Car-Parrinello method [7] essentially solves the many-electron Schrödinger equation in the Born-Oppenheimer approximation for the ground state for every time step, using a local density functional Hamiltonian.

Quantum dynamical simulations provide a complete

solution of the time dependent Schrödinger equation for one or more quantum particles in an environment of classical particles. Wave packet propagation [8] falls into this category. The method of Selloni *et al.* [9] describes the wave function on a grid and solves the time dependent Schrödinger equation by a split operator technique. The method is more general and could be employed for reactive processes. The method of Selloni *et al.* is in its original form restricted to the ground state Born-Oppenheimer surface. Very recently a surface-hopping method was applied to study nonadiabatic transitions of a solvated electron, based on the scheme of Selloni *et al.* [10–12]. In this case the method seemed to correctly predict the probabilities for nonadiabatic transitions, mainly due to the large energy gap between the states and hence low probabilities of hopping.

A density-matrix evolution (DME) method was recently developed by us. The method is capable of blending classical and quantum degrees of freedom in MD simulations, while conserving the total energy. Its detailed description is given elsewhere [13]. The DME method was applied to nonadiabatic intramolecular proton transfer in an aqueous solution [14].

Collisions between a quantum harmonic oscillator (QHO) and classical noble-gas atoms were studied by several authors [13,15,16]. These studies were restricted to a single noble-gas atom and to collinear collisions. Herman and Berne [17] studied the influence of a noble-gas bath on the vibrational spectrum of diatomics by Monte Carlo simulations. Berens and co-workers [18,19] simulated vibrational and rotational spectra of diatomics embedded in an argon bath by classical molecular dynamics and analytical quantum corrections. Lynch *et al.* [20] studied by MD the vibrational spectra of hydrogen adsorbed on Ni and Pd surfaces. A QHO immersed in a noble-gas bath is a typical system where the argon atoms are described with sufficient accuracy by the laws of classical mechanics, while the QHO itself requires a quantum description. The model is a prototype for energy transfer from translational to vibrational degrees of freedom and with modifications of the potential the model can be ap-

\*Permanent address: National Institute of Chemistry, P.O.B. 30, Hajdrihova 19, 61115, Ljubljana, Slovenia.

†To whom correspondence should be addressed.

plied to proton tunneling in hydrogen bonds or to charge transfer reactions.

We put a QHO at the center of the simulation box, surrounded it with Lennard-Jones atoms, and applied periodic boundary conditions. We avoided quantum or classical treatment of rotations and translations of the harmonic oscillator by fixing the QHO to the center of the simulation cell and allowed vibrations to take place only in the  $x$  direction. The QHO was approximated by expanding its wave function in the three lowest eigenstates and its dynamics was described by density-matrix evolution equations, while for the noble-gas atoms classical equations of motion were assumed. The quantum and classical subsystems were properly coupled and the differential equations were integrated simultaneously. Conservation of total energy was observed for a molecular dynamics simulation of QHO and classical noble-gas atoms when no coupling to a temperature bath was applied.

The outline of this article is as follows. Section II describes the computational methods. Section III reports the results of simulations using (i) a QHO immersed in a diluted noble gas and (ii) a QHO immersed in a dense noble gas. In Sec. IV some concluding remarks are given.

## II. COMPUTATIONAL METHODS

The DME method, introduced recently into MD by Berendsen and Mavri, is described in detail elsewhere [13]. Here we give only the basic ideas underlying the method.

The wave function of the quantum subsystem is expanded on a properly chosen orthonormal basis set of basis functions  $\phi$ :

$$\psi(\xi, t) = \sum_{n=1}^M c_n(t) \phi_n(\xi), \quad (1)$$

where  $\xi$  denotes the coordinates of the quantum subsystem. The  $M \times M$  density matrix  $\rho$  is defined as  $\rho_{nm} = c_n c_m^*$ . When  $\phi_n$  are chosen as eigenfunctions of the unperturbed quantum oscillator, each  $n$  can be identified with a quantum level. The  $n$  level system can be described by the time dependent density matrix  $\rho$  with dimension  $n \times n$ . Note that the matrix  $\rho$  is complex but Hermitian. Diagonal elements of the density matrix represent populations of the levels, while the off-diagonal elements contain phase information. A suitable choice for the initial condition of the density matrix is  $\rho_{11} = 1$ , and all other elements zero, implying that the quantum subsystem is initially in its ground state, with unspecified phase.

If necessary, the basis functions are orthogonalized. In the present case, the latter step can be avoided, since the basis set we use consists of Gauss-Hermite functions, which are exact solutions of the unperturbed harmonic oscillator. In the present study we applied the first three Gauss-Hermite functions for a three level QHO and therefore a minimal basis set was used. The  $\mathbf{H}^0$  matrix elements can be calculated analytically, where

$H_{n,m}^0 = \langle n | H^0 | m \rangle$  and  $H^0$  stands for the Hamiltonian of the unperturbed harmonic oscillator. Note that  $\mathbf{H}^0$  is diagonal with the elements corresponding to the energies of the unperturbed quantum harmonic oscillator, i.e.,  $E_k = (k + 1/2)\hbar\omega$  and  $k = 0, 1, 2$ .

From positions of the classical particles acting on the harmonic oscillator the perturbation Hamiltonian matrix elements can be calculated from

$$H'_{n,m} = \sum_{i=1}^N \langle n | H'_i | m \rangle, \quad (2)$$

where  $H'_i$  stands for the interaction between the quantum and the  $i$ th classical particle and the sum runs over  $N$  classical atoms. A pair-additive interaction energy between the QHO and classical noble-gas atoms was assumed. The matrices  $\mathbf{H}^0$  and  $\mathbf{H}'$  are summed and the Hamiltonian matrix is calculated,  $\mathbf{H} = \mathbf{H}^0 + \mathbf{H}'$ . The energy of the quantum subsystem can be immediately calculated,

$$E_Q = \text{Tr}(\rho \mathbf{H}). \quad (3)$$

Note that diagonalization of  $\mathbf{H}$  is not required.

In order to couple the classical degrees of freedom with the quantum subsystem it is necessary to calculate the forces on the classical particles. Matrix elements for calculation of the Hellmann-Feynman force are defined as

$$F_{nm,u} = \left\langle n \left| -\frac{\partial H}{\partial u} \right| m \right\rangle, \quad (4)$$

where  $u$  stands for the directions  $x$ ,  $y$ , and  $z$ , respectively, on each classical particle. The force acting from the quantum subsystem on a classical particle in the  $u$  direction is

$$F_u^Q = \text{Tr}(\rho \mathbf{F}_u). \quad (5)$$

The quantum force component was added to the classical force,

$$\mathbf{F}_u = F_u^Q - \sum_{j \neq i}^N \frac{\partial V_{i,j}}{\partial u}, \quad (6)$$

and this total force is used to update the velocity and position of the classical particle.

The density matrix evolves with time according to the Liouville-von Neumann equation [21]

$$\frac{d}{dt} \rho = \frac{i}{\hbar} (\rho \mathbf{H} - \mathbf{H} \rho). \quad (7)$$

The system of differential equations for the DME and equations of motion for the classical particles are integrated simultaneously. The MD scheme is somewhat related to the method of Selloni *et al.* [9], but an important advantage is that excited states and hence nonadiabatic transitions can be treated.

To summarize the DME-MD scheme, the classical sub-

system is coupled to a quantum subsystem by forces that are different for various quantum states, while the quantum subsystem is coupled to classical degrees of freedom by changes in  $\mathbf{H}'$ . The equations of motion ensure that total energy is conserved [13]. In the case that the basis functions are restricted to a description of the ground state the method becomes adiabatic, i.e., dynamics is restricted to a single Born-Oppenheimer surface and can be related to recent adiabatic studies of proton transfer reactions [22,23].

We modeled the quantum harmonic oscillator in one dimension along the  $x$  axis. We considered only deviations from the equilibrium bond length described by a quantum coordinate  $\xi = r - r_0$ , where  $r_0$  is the equilibrium bond length of the oscillator. The mass of the oscillator and a force constant were chosen in such a way that the frequency of the unperturbed oscillator was  $1000 \text{ cm}^{-1}$ , corresponding to a typical chemical bond stretching frequency. When integrating the equations of motion, the position of the quantum oscillator remained fixed at the center of the simulation cell. An appropriate picture of the system is a single chemical bond stretching on the surface of a macromolecule or (chemi)sorbed molecule on a catalyst's surface. By transformations given elsewhere [16] one can cast the model into a vibrating diatomic molecule with appropriate scaling of reduced mass and force constant.

The interaction energy between QHO and noble-gas atoms was described by a Buckingham potential  $V = Ae^{-br}$ , since calculations of the integrals using series expansion (see Appendix) are relatively easy with this functional form of the potential function. Values of parameters were  $A = 1 \times 10^5 \text{ kcal/mol}$  and  $b = 4 \text{ \AA}^{-1}$ . Forces between QHO and atoms constituting the bath were therefore repulsive for all distances. The interaction energy between noble-gas atoms was described by a Lennard-Jones potential  $V = 4\epsilon(\sigma^{12}/r^{12} - \sigma^6/r^6)$  with  $\sigma = 3.405 \text{ \AA}$  and  $\epsilon = 0.23845 \text{ kcal mol}^{-1}$ , corresponding to the values for argon.

Equations of motion and DME equations were integrated simultaneously by the fourth order Runge-Kutta method with a time step of 0.1 fs for 20 ps. MD was carried out at constant temperature and constant volume. The algorithm of Berendsen *et al.* [24] was applied for the temperature coupling to a bath with a temperature of 1000 K with a coupling time constant of  $\tau_T = 50 \text{ fs}$ . The main reason for performing the simulations at 1000 K was that at this elevated temperature excited states are more populated than at room temperature, which makes the analysis more reliable. In addition, at elevated temperature the relaxation time of the system is shorter, which allows the use of shorter equilibration time. MD simulations were performed at constant volume, using a cubical simulation box with edge length of  $15 \text{ \AA}$ . Periodic boundary conditions with a spherical cutoff of  $7.5 \text{ \AA}$  were applied for the calculations of forces and interaction energies. We used two densities: a system of 27 atoms corresponding to a reduced density of 0.316 and a system of 80 atoms corresponding to 0.936. The densities can be compared with the experimental solid triple point density of argon of 0.9647 [25].

### III. RESULTS AND DISCUSSION

The time evolution of the diagonal elements of the density matrix for a three level QHO in a bath of 26 Ar atoms is shown in Fig. 1. Individual collisions of noble-gas atoms with the QHO can be observed as separate dips in the ground state populations and peaks in excited state populations. Since most of the collisions are elastic and only a few collinear collisions were observed in the simulation time due to the low density, the equilibrium was not achieved during the 20 ps MD run. By increasing the number of Ar atoms to 79 a rapid decay of the ground state population and a simultaneous increase of the excited state population were achieved in the first couple of hundred femtoseconds (Fig. 2). Quantities were analyzed between 2 ps and 20 ps. Average values of the populations are given in Table I. Time-averaged populations appear to be Boltzmann distributed. Time averages of the diagonal elements of the density matrix can be compared with calculated populations (i) assuming that during the MD the quantum levels are fixed to their unperturbed values, which leads to an analytical expression and (ii) taking into account the shifted energy eigenvalues obtained by diagonalization of the Hamiltonian in MD. Using eigenvalues from MD the average Boltzmann factor and associated free energy differences between the vibrational states of the QHO were calculated. Free energy differences (Table I) reveal that in a simulated system the spacing between the levels in terms of free energies increases relative to the *in vacuo* value. It is worth mentioning that the first method represents an approximation that is valid if the perturbation of the quantum system by the environment is weak, while the second method is exact in the thermodynamic limit.

From the expectation values of the displacement  $\xi$  the vibrational spectrum was calculated by fast Fourier

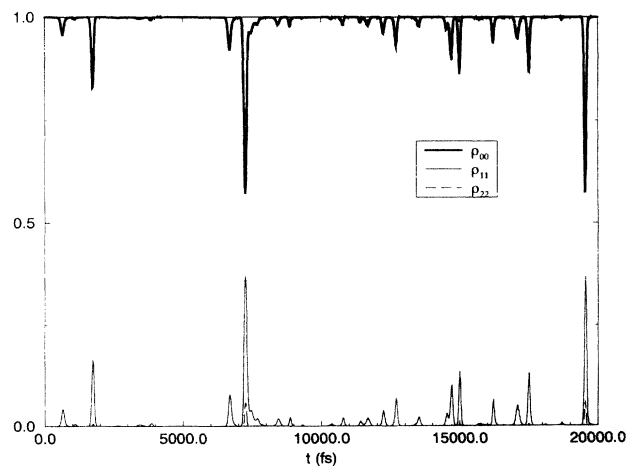


FIG. 1. Time evolution of the diagonal elements of the density matrix for a three level quantum harmonic oscillator in a diluted Ar bath at 1000 K (26 Ar atoms in a simulation box of  $15 \text{ \AA} \times 15 \text{ \AA} \times 15 \text{ \AA}$ ): ground state  $\rho_{00}$  (thick solid line), first excited state  $\rho_{11}$  (thin solid line), and second excited state  $\rho_{22}$  (dashed line).

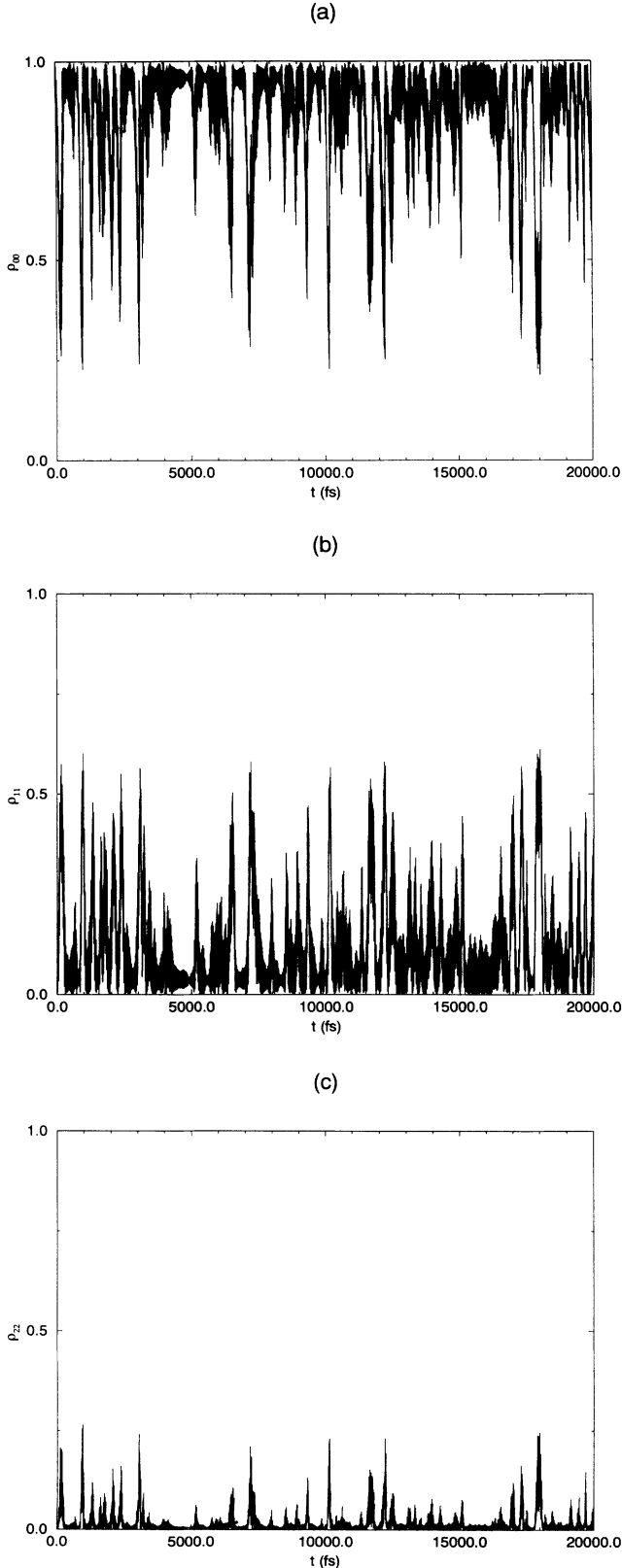


FIG. 2. Time evolution of the diagonal elements of the density matrix for a three level quantum harmonic oscillator in a dense Ar bath at 1000 K (79 Ar atoms in a simulation box of  $15 \text{ \AA} \times 15 \text{ \AA} \times 15 \text{ \AA}$ ): ground state  $\rho_{00}$  (a), first excited state  $\rho_{11}$  (b), and second excited state  $\rho_{22}$  (c).

TABLE I. Populations of vibrational levels of a perturbed quantum harmonic oscillator in a dense Ar bath at a temperature of 1000 K. (a) Time average from the molecular dynamics run between 2 ps and 20 ps. (b) Analytically calculated from Boltzmann distribution by assuming that the collisions do not shift the equidistant vibrational levels, which are those of the unperturbed oscillator. (c) As in (b) but taking into account MD-calculated averaged Boltzmann factors in the interval between 2 ps and 20 ps. The values for  $-kT \ln \langle \exp[-(E_1 - E_0)/kT] \rangle$  and  $-kT \ln \langle \exp[-(E_2 - E_0)/kT] \rangle$  were  $3.21 \text{ kcal mol}^{-1}$  and  $6.99 \text{ kcal mol}^{-1}$ , respectively, which can be compared with the *in vacuo* values of  $2.86 \text{ kcal mol}^{-1}$  and  $5.72 \text{ kcal mol}^{-1}$ . Errors evaluated from 2 ps subaverages are given in parentheses, and have been calculated according to  $\{\sum_{i=1}^S (x_i - \bar{x})^2 / [S(S-1)]\}^{1/2}$ . Herein  $S$  is the number of subaverages and  $\bar{x}$  is the average over subaverages  $x_i$ .

Method	$\rho_{00}$	$\rho_{11}$	$\rho_{22}$
MD (a)	0.864(0.012)	0.122(0.010)	0.018(0.002)
(b)	0.773	0.183	0.043
(c)	0.814	0.162(0.004)	0.024(0.002)

transform (FFT). Here we apply linear response theory, which predicts proportionality between the experimental vibrational spectrum and the power spectrum of the Fourier transformed time course of the vibrational coordinate multiplied with a factor proportional to  $\omega$  [18,26]. Note that the factor  $(1 - \exp^{-\hbar\omega/k_B T})$  implying the thermal equilibrium between the ground state and excited states is already implicitly included in the DME equations. We assume that changes in the dipole moment (for infrared spectra) or changes in polarizability (for Raman spectra) are proportional to  $\xi$ . Since the value of the factor  $\omega$  is one to two orders of magnitude lower at frequencies between 0 and  $200 \text{ cm}^{-1}$ , corresponding to vibrational modes between the QHO and noble-gas atoms, than at the resonance frequency, the simulated band in the low frequency region is weak. We would like to stress that in our MD simulations coordinate origin and orientation of the QHO were constrained. Therefore the contributions to the spectrum due to rotation, corresponding to low frequencies, were not taken into account. In addition, no filtering techniques were applied in FFT and we are aware that some artifacts due to truncation and insufficient statistics are possible [18].

The simulated spectrum is shown in Fig. 3. A blueshift with distorted symmetry is evident for the  $1000 \text{ cm}^{-1}$  peak. In addition, a weak band appeared at frequencies around  $100 \text{ cm}^{-1}$ , corresponding to the intermolecular mode of QHO and colliding noble-gas atoms. This low frequency mode has the classical analogy of response of a diatomic to a collinear collision with a noble-gas atom by shrinking the bond length.

The spectrum can be compared qualitatively with the experimental and simulated infrared and Raman spectra of diatomics in an argon bath [17–19]. It is worthwhile to emphasize that neither the experiments nor the previous simulations were performed at such a high temperature. In addition, contributions due to rotations of a

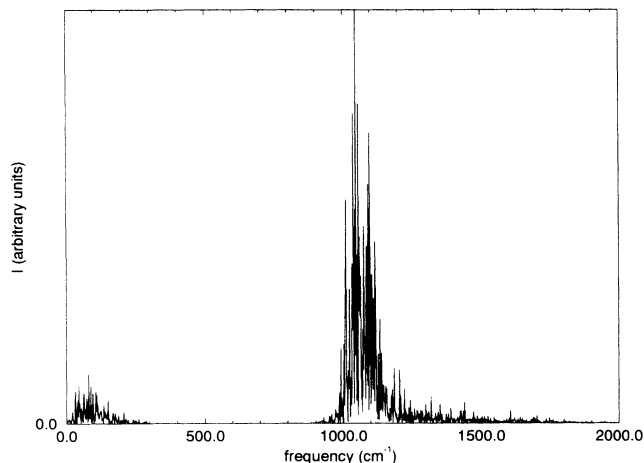


FIG. 3. Power spectrum of the Fourier transform of the expectation value of  $\xi$  multiplied by  $\omega$  for a quantum harmonic oscillator and 79 Ar atoms. Note that the vibrational frequency of the unperturbed oscillator is  $1000 \text{ cm}^{-1}$ . Abscissa is given in  $\text{cm}^{-1}$ , while the intensity is in arbitrary units.

QHO are missing in our simulated spectrum. In a simulated isotropic Raman spectrum of  $\text{Br}_2$  in an Ar bath by Monte Carlo techniques [17] a blueshift with distorted symmetry was observed. The blueshift increases by increasing the argon density at the densities that are comparable with our study. For very low densities a redshift was predicted.

An additional comparison can be made with the experimental [27,28] and carefully simulated [18] spectrum of carbon oxide in an argon bath. Fundamental vibrational-rotational bands with two peaks were observed *in vacuo* and at low Ar densities and their coalescence is observed at higher Ar densities. Experimental studies in dense Ar were performed at temperatures of 97 K [27] and 298 K [28].

The authors report an extreme sensitivity of the simulated spectrum to the choice of the nonbonding parameters in simulations. They obtained agreement with experiment only if different nonbonding parameters were applied for the ground and excited vibrational states [17]. Since in our study the interaction energy between the QHO and the bath atoms was only repulsive, no rotations of the QHO were allowed, and our study was performed at 1000 K, good agreement with the available experimental spectra cannot be expected.

The noble-gas atoms dynamics could be integrated with a time step at least two orders of magnitude larger, but since the DME equations require a time step of 0.1 fs the time step for the integration of the overall system was taken as 0.1 fs. In the present case the straightforward usage of the multiple time step MD scheme, as in the method of Selloni *et al.*, is not applicable. A possible implementation of the multiple time step MD would be the integration of the quantum subsystem and the first solvation shell of the noble gas with a short time step and the rest of the system with a longer time step. The time course of the density-matrix elements reveals that

they are rapidly oscillating functions with a frequency corresponding to the instantaneous spacing between the levels, which is most of the time close to the frequency of the unperturbed oscillator. In future applications it would be worthwhile to transform the DME equations to eliminate the frequency of the unperturbed quantum oscillator, which can be related to the rotating frame concept in the theory of nuclear magnetic resonance [29]. We expect that by inclusion of higher quantum levels even a higher order expansion in terms of  $\xi$  would be necessary or numerical calculation of the integrals would be necessary, as was performed in an adiabatic MD study of the proton transfer process [22].

#### IV. CONCLUSIONS

Molecular dynamics simulation of a system with mixed classical and quantum degrees of freedom was performed by coupling classical and quantum degrees of freedom by the density-matrix evolution (DME) method. In the quantum MD scheme using the DME method, the classical subsystem is coupled to a quantum subsystem by forces that are different for various quantum states, while the quantum subsystem is coupled to classical degrees of freedom by changes in  $\mathbf{H}'$ , which enters the DME equations. The forces on the classical degrees of freedom are computed from a series expansion in the quantum coordinates. Due to the fact that the calculations are based on a limited set of basis functions, the DME method seems to be the most suitable for quantum simulations of nuclear degrees of freedom, where the energy levels are relatively close to each other and the wave function is localized, and for electronically excited states of molecules.

Populations of the vibrational levels of a quantum harmonic oscillator are close to the Boltzmann distribution. We have simulated the equilibrium distribution of quantum level populations using nonadiabatic quantum molecular dynamics. From the averaged Boltzmann factor the free energy for the transfer from ground to the excited vibrational levels was calculated and was found to be larger than the corresponding *in vacuo* value. We believe that a discrepancy between the populations calculated by free energy differences and by MD averages originates from the numerical errors introduced by series expansion calculations of the integrals.

In the calculated vibrational spectrum of the harmonic oscillator in the noble-gas bath at 1000 K a blueshift and distorted symmetry, with a more intensive wing in the direction of higher frequencies, were observed for the band corresponding to the intramolecular vibrations. A weak band was observed at about  $100 \text{ cm}^{-1}$  corresponding to intermolecular modes. The blueshift results from the perturbation of the oscillator by the repulsive interaction with Ar atoms.

The DME approach seems to be readily applicable to molecular dynamics simulations of complex systems, where a few degrees of freedom must be treated by quantum mechanics, while the rest of the system is described with sufficient accuracy by the laws of classical mechanics. We demonstrated by MD-DME simulation that

populations of the quantum harmonic oscillator levels obey the Boltzmann distribution law. This is an additional proof that coupling between the quantum subsystem and the classical subsystem was realized properly. Future work will be directed toward more complex applications, such as reaction dynamics of proton transfer or charge transfer processes. In addition, the DME method can easily incorporate an external field. It is a suitable method for computational support of femtosecond spectroscopy, since it can easily simulate optical dephasing and pulse echo experiments.

### ACKNOWLEDGMENTS

One of us (J.M.) is grateful for financial aid from The Ministry of Science and Technology of the Republic of Slovenia and to the University of Groningen for the hospitality during his stay in The Netherlands.

### APPENDIX

The details of the calculations of different matrix elements used for the calculation of  $\mathbf{H}$  and of the Hellmann-Feynman force will be presented here. The first three Gauss-Hermite functions are

$$\Phi_1 = N_1 \exp(-\alpha \xi^2), \quad (\text{A1})$$

$$\Phi_2 = N_2 2y \exp(-\alpha \xi^2), \quad (\text{A2})$$

$$\Phi_3 = N_3 (4y^2 - 2) \exp(-\alpha \xi^2), \quad (\text{A3})$$

where  $y = \xi(m\omega/\hbar)^{1/2}$ . If  $\xi$  is given in  $\text{\AA}$  then  $y = 5.4475315 \xi$ . For a  $1000 \text{ cm}^{-1}$  oscillator the value of the exponent is fixed  $\alpha = 14.8378 \text{ \AA}^{-2}$ .

The contribution to the matrix element due to perturbation of the QHO by a single noble-gas atom is given by

$$\begin{aligned} H'_{n,m} &= \int_{\xi=-\infty}^{\infty} \Phi_n(\xi) A \\ &\times \exp\{-b[(x-\xi)^2 + y^2 + z^2]^{1/2}\} \\ &\times \Phi_m(\xi) d\xi, \end{aligned} \quad (\text{A4})$$

where it is assumed that the QHO was positioned at the local coordinate system origin and  $x, y, z$  are the Carte-

sian coordinates of a noble-gas atom. Note that the equation above corresponds to the individual summation terms in Eq. (2). The integral can be calculated analytically only if simultaneously  $y = 0$  and  $z = 0$ . Due to the fact that the probability density of the quantum particle  $\xi$  is narrow and is centered around  $\xi = 0$ , a series expansion of the term  $A \exp\{-b[(x-\xi)^2 + y^2 + z^2]^{1/2}\}$  can be performed with respect to  $\xi$  around  $\xi = 0$ .

By introducing a new variable  $r = (x^2 + y^2 + z^2)^{1/2}$  the term  $V' = A \exp\{-b[(x-\xi)^2 + y^2 + z^2]^{1/2}\}$  reads, after the expansion and rearrangement,

$$V' \approx Ae^{-br} + \lambda_1 \xi + \lambda_2 \xi^2 + \lambda_3 \xi^3, \quad (\text{A5})$$

where

$$\lambda_1 = Ae^{-br} \frac{b|x|}{r}, \quad (\text{A6})$$

$$\lambda_2 = \frac{1}{2} Ae^{-br} \left( \frac{b^2 x^2}{r^2} + \frac{bx^2}{r^3} \right), \quad (\text{A7})$$

$$\lambda_3 = \frac{1}{6} Ae^{-br} \left( \frac{b^3 |x|^3}{r^3} + \frac{3b^2 |x|^3}{r^4} + \frac{3b |x|^3}{r^5} \right). \quad (\text{A8})$$

An important advantage is that the integral can now be expressed in terms of integrals  $\langle m|n \rangle$ ,  $\langle m|\xi|n \rangle$ ,  $\langle m|\xi^2|n \rangle$ , and  $\langle m|\xi^3|n \rangle$  that are independent of the positions of classical particles and are thus calculated prior to the MD run and stored.

With the same procedure the matrix elements for the Hellmann-Feynman force are calculated for each term in Eq. (4). The Hellmann-Feynman forces' matrix elements read

$$F'_u \approx bAu \left( \frac{e^{-br}}{r} + \mu_1 \xi + \mu_2 \xi^2 + \mu_3 \xi^3 \right), \quad (\text{A9})$$

where

$$\mu_1 = \frac{|x| e^{-br}}{r^2} \left( b + \frac{1}{r} \right), \quad (\text{A10})$$

$$\mu_2 = \frac{|x^2| e^{-br}}{2} \left( \frac{b^2}{r^3} + \frac{3b}{r^4} + \frac{3}{r^5} \right), \quad (\text{A11})$$

$$\mu_3 = \frac{|x^3| e^{-br}}{6} \left( \frac{b^3}{r^4} + \frac{6b^2}{r^5} + \frac{15b}{r^6} + \frac{15}{r^7} \right), \quad (\text{A12})$$

and  $u$  stands for  $x, y$ , and  $z$ , respectively, and  $r$  is again  $(x^2 + y^2 + z^2)^{1/2}$ .

- [1] R.P. Feynman and A.R. Hibbs, *Quantum Mechanics and Path Integrals* (McGraw-Hill, New York, 1965).
- [2] M.J. Gillan, *Philos. Mag. A* **58**, 257 (1988).
- [3] G.A. Voth, D. Chandler, and W.H. Miller, *J. Chem. Phys.* **91**, 7749 (1989).
- [4] C.H. Mak, *Phys. Rev. Lett.* **68**, 899 (1992).
- [5] C. H. Mak and J.N. Gehlen, *Chem. Phys. Lett.* **206**, 130

(1993).

- [6] T.R. Mattson, V. Engberg, and G. Wahnstrom, *Phys. Rev. Lett.* **71**, 2615 (1993).
- [7] R. Car and M. Parrinello, *Phys. Rev. Lett.* **55**, 2471 (1985).
- [8] E.J. Heller, *J. Chem. Phys.* **62**, 1544 (1975); K. Singer and W. Smith, *Mol. Phys.* **57**, 761 (1986).

- [9] A. Selloni, P. Carnevali, R. Car, and M. Parrinello, *Phys. Rev. Lett.* **59**, 823 (1987).
- [10] F. Webster, P.J. Rosky, and R.A. Friesner, *Comput. Phys. Commun.* **63**, 494 (1991).
- [11] B. Space and D.F. Coker, *J. Chem. Phys.* **94**, 1976 (1991).
- [12] B. Space and D.F. Coker, *J. Chem. Phys.* **96**, 652 (1992).
- [13] H.J.C. Berendsen and J. Mavri, *J. Phys. Chem.* **97**, 13464 (1993).
- [14] J. Mavri, H.J.C. Berendsen, and W.F. van Gunsteren, *J. Phys. Chem.* **97**, 13469 (1993).
- [15] D. Rapp and T.E. Sharp, *J. Chem. Phys.* **38**, 2641 (1963).
- [16] D. Secrest and B.R. Johnson, *J. Chem. Phys.* **45**, 4556 (1966).
- [17] M.F. Herman and B.J. Berne, *J. Chem. Phys.* **78**, 4103 (1983).
- [18] P.H. Berens and K.R. Wilson, *J. Chem. Phys.* **74**, 4872 (1981).
- [19] P.H. Berens, S.R. White, and K.R. Wilson, *J. Chem. Phys.* **75**, 515 (1981).
- [20] D.L. Lynch, S.W. Rick, M.A. Gomez, B.W. Spath, J.D. Doll, and L.R. Pratt, *J. Chem. Phys.* **97**, 5177 (1992).
- [21] E. Merzbacher, *Quantum Mechanics* (Wiley, New York, 1970).
- [22] D.C. Borgis, G. Tarjus, and H. Azzouz, *J. Phys. Chem.* **96**, 3188 (1992).
- [23] D. Laria, G. Ciccotti, M. Ferrario, and R. Kapral, *J. Chem. Phys.* **97**, 378 (1992).
- [24] H.J.C. Berendsen, J.P.M. Postma, W.F. van Gunsteren, A. DiNola, and J.R. Haak, *J. Chem. Phys.* **81**, 3684 (1984).
- [25] J.H. Holloway, *Noble-Gas Chemistry* (Methuen, London, 1968).
- [26] D. A. McQuarrie, *Statistical Mechanics* (Harper and Row, New York, 1976), pp. 467-592.
- [27] U. Buontempo, S. Cunsolo, and G. Jacucci, *J. Chem. Phys.* **59**, 3750 (1973).
- [28] R. Coulon, L. Galatry, B. Okseengorn, S. Rubin, and B. Vodar, *J. Phys. Radium*, **15**, 641 (1954).
- [29] R.R. Ernst, G. Bodenhausen, and A. Wokaun, *Principles of Nuclear Magnetic Resonance in One and Two Dimensions* (Clarendon Press, Oxford, 1987).